

H14-293 CAPABILITY OF THE STANDARD (K,ε) MODEL FOR SIMULATING ATMOSPHERIC DISPERSION OVER A NPP SITE

Pierre Roubin and Franck Jourdain

Commissariat à l'Énergie Atomique, Direction de l'Énergie Nucléaire (CEA/DEN), France

Abstract: The dispersion of a tracer gas at the Bugey NPP site was simulated in the LMFA wind tunnel at Université Lyon 1 with the financial support of the IRSN. The measurements were available in four flow configurations and used to assess the capability of basic turbulence modelling of a general CFD software, in this instance STAR-CD, to predict the flow velocity and gas concentration in the wake of the building canopy with the standard (k,ε) turbulence model.

Following a short description of the site topographical characteristics and of the experiment, the corresponding numerical modelling with STAR-CD is outlined and the comparison of its predictions with the measurements is commented on for a neutrally stable boundary layer.

The main flow characteristics, which depend on the wind direction and tracer gas source location, are qualitatively well captured by the CFD simulations. From the quantitative point of view, the ground level concentration is underpredicted on the first hundred metres and conversely overpredicted beyond, which is attributed to the overestimation of the initial plume height by the stack release and underestimation of lateral plume spread by the (k,ε) model. Nevertheless the discrepancy between measurement and prediction is less than a factor of two, which shows that a rather simple CFD model can yield useful results for many practical applications in environmental impact or risk management of industrial sites.

Key words: environmental impact, air pollution, atmospheric dispersion, wind engineering, near field, (k,ε) turbulence model.

INTRODUCTION

The near field dispersion of a tracer gas at the Bugey nuclear power plant site was simulated in the wind tunnel of the Laboratoire de Mécanique des Fluides et d'Acoustique (LMFA-UMR CNRS 5509, ECL, Université Lyon 1) under funding from the Institut de Radioprotection et Sécurité Nucléaire (IRSN). The measurements were available in four flow configurations and used here to assess the capability of a general CFD software, in this instance STAR-CD, when used with basic modelling options to predict the velocity pattern and distribution of the gas concentration in the wake of the building canopy of an industrial site.

EXPERIMENT

Tests were made by Méjean (2005) on a 1/500 scaled down model of the Bugey site installed in the LMFA wind tunnel, whose test section is 3.7 m wide, 2 m high and 14 m long (fig.1). Turbulence generators allow reproducing realistic boundary layer wind profiles in neutral stability conditions, with air temperature maintained constant during the tests.



Figure 1. Bugey model in LMFA test section

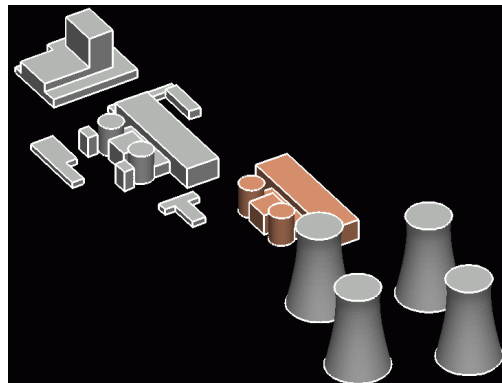


Figure 2. Building geometry simulated in STAR-CD

Model configuration

The Bugey NPP comprises five reactors, one decommissioned gas cooled reactor (UNGG type), whose main building is 82 m high, and four pressurised water reactors (PWR) each associated to a 140 m high cooling tower (fig.2). These are surrounded by numerous lower height buildings, all situated in the agricultural plain of the Rhône valley on almost flat terrain remote from neighbouring relief or other high constructions.

Flow conditions

A 3.7 ms^{-1} wind speed at 50m elevation was considered from the north and the south, which are the dominant wind directions at the site. For each direction two types of tracer gas (ethane) sources were considered:

- i) Surface source simulating $16700 \text{ m}^3\text{h}^{-1}$ uniformly transpiring all over the south containment building wall (50m high),
- ii) Punctual source simulating a $28000 \text{ m}^3\text{h}^{-1}$ ventilation exhaust at the south stack 55 m high and 2.2 m diameter.

Similarity

The test section was operated in ambient conditions so as to respect the similarity of the velocity field, resulting in a Reynolds number distortion of 1/500 identical to the model reduction scale. Consequently artificial ground roughness was introduced to maintain longitudinally a vertical wind profile identical to that measured in situ. Note that whereas pure ethane

could be injected in the case of the leaking containment release at low flow rate, it had to be diluted with air in the case of stack release to achieve the 20.5 ms⁻¹ exit velocity of the mixture. The corresponding modification of the ethane concentration at this boundary was accounted for in the numerical simulation to allow direct comparison with the measurements.

Measurements

Using a laser light plane, many cross sections helped visualise and understand the live flow pattern. For post-test analysis a large amount of data is referenced in a local coordinate system centred on the south containment building with OX, OY and OZ axis respectively oriented towards the east, north and upward:

- i) LDA measurements provide mean values of the three velocity components plus the fluctuations variance of the longitudinal (OY oriented) instant velocity. Both vertical profiles in the X=0 plane and parallel to OX horizontal profiles at 4 heights above the ground are recorded for 15 longitudinal positions.
- ii) The ethane instantaneous concentration was measured with a carefully calibrated flame ionisation technique, which allowed obtaining mean concentration profiles at similar locations to the velocity and up to 2000 m downstream of the release point. The background ethane pollution due to continuous injection during each test was of course subtracted from the raw signal to get the actual concentration.

NUMERICAL MODEL

Here under is defined how a “simple” model was set up within STAR-CD. All computations are steady state runs. Convergence to a 10⁻⁴ residual requires 300 to 3000 iterations depending on the combination of mesh size, numerical scheme and flow configuration chosen.

Computational domain and mesh

Only the largest buildings are represented and lay on flat terrain. Horizontally the domain extent depends on the wind direction as indicated in table 1.

Table 3. Domain spatial extent

Wind from	X _{min} /X _{max} (m)	Y _{min} /Y _{max} (m)	Z _{min} /Z _{max} (m)
South	-500/500	-550/2500	0/300
North	-500/500	-2150/1050	0/300

The corresponding meshes comprise 4.5 10⁵ to 6.5 10⁵ cells for the containment and stack release case respectively, the latter requiring additional local refinement to describe the stack jet expansion and curvature before it expands into a wider plume. Cells are mostly hexahedrons (95%) as grid lines are aligned with the main flow direction. Typical cell sizes away from walls range from 0.3 m at the stack exit to 40 m at the domain lateral or top boundaries. Wall cell thickness varies from 0.15 m on buildings to 0.5 m at the ground boundary.

Turbulence modelling

These computations employed the standard form of the Launder and Spalding (1972) (k,ε) turbulence model, where the turbulent fluxes of scalar variables $\overline{u_i'c'}$ are simply modelled with proportionality to the mean concentration gradient:

$$\overline{u_i'c'} = \frac{-v_t}{Sc_t} \cdot \frac{\partial \overline{C}}{\partial x_i} \quad (1)$$

with $v_t = k^2/\epsilon$ turbulent viscosity and Sc_t turbulent Schmidt number of 0.9

Boundary conditions

The conditions at the domain upstream boundary conform to the set proposed by Richards and Hoxey (1993) that guaranties the longitudinal homogeneity of the flow away from obstacles.

$$\text{longitudinal velocity} \quad \frac{V(z)}{u^*} = \frac{1}{\kappa} \text{Ln}\left(\frac{z}{z_0}\right) \quad (2)$$

$$\text{turb. kin. energy} \quad k(z) = \frac{u^{*2}}{\sqrt{C_\mu}} \quad (3)$$

$$\text{dissipation of k} \quad \epsilon(z) = \frac{u^{*3}}{\kappa \cdot z} \quad (4)$$

with u^* friction velocity, κ the Von Karman constant and $C_\mu = 0.013$

Other lateral walls of the domain are set far enough from the building influence to apply uniform pressure at the downstream boundary and symmetry at both lateral boundaries. U, k and ε are imposed on the top boundary at their respective value given by equations (2) to (4) for $z = Z_{\text{max}}$. On solid boundaries wall functions apply, that of smooth walls for buildings and that of rough walls for the ground. As pointed out by Hargreaves and Wright (2007) the rugosity height input to the STAR-CD wall function treatment has to be corrected to represent the aerodynamic roughness simulated in the wind tunnel, this was done as demonstrated by Blocken, Stathopoulos and Carmeliet (2007).

RESULTS AND DISCUSSION

The plume behaviour obviously depends on the wind direction and on the spatial extent of the tracer source:

- Stack release occurring in a high velocity zone aloft is barely influenced by the buildings canopy except by the high cooling towers; conversely the simulation of a uniformly leaking PWR containment building concerns a lower velocity zone near the ground and is affected by even the lower building wakes.
- When wind blows from the south, the only obstacle is the UNGG building. Its location relative to the source does not significantly alter the wind profile from the open field situation upstream; conversely the screen of the four cooling towers constitutes a major disturbance when wind blows from the north.

Release from the containment building

Under south wind, the shape and ranking of the vertical profiles as a function of the downwind distance along axis OY (figure 3) qualitatively conforms to the experiment, but the altitude of the maximum concentration is predicted about 10 metres too high, resulting in underprediction (typically -20% to -50%) of the ground level concentration in the built area. Beyond the cooling towers ($Y > 800$ m), the predicted decay of the ground concentration follows the experimental trend, exceeding the measured value by less than a factor of two for both wind directions (figure 4).

Under north wind, the release occurs in the wake of the cooling towers that produce a large scale mixing, consequently profiles no longer have their maximum aloft and concentration continuously decreases with altitude. The ground concentration is slightly underpredicted by 20% on the first four hundred meters (figure 4). The span wise spread of the plume is also underpredicted beyond one kilometre downstream from the source (figure 5).

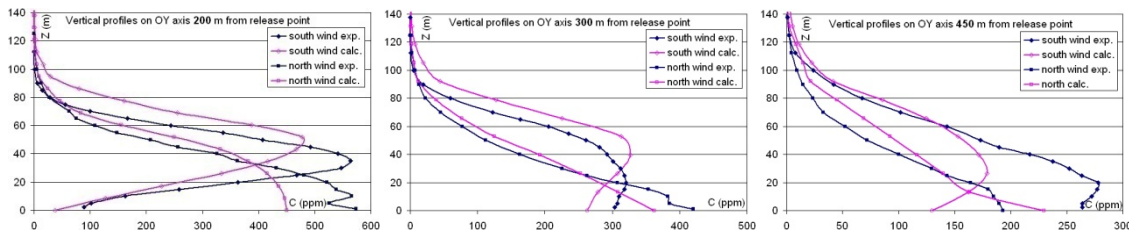


Figure 3. Vertical concentration profiles at 3 distances from the leaking containment building

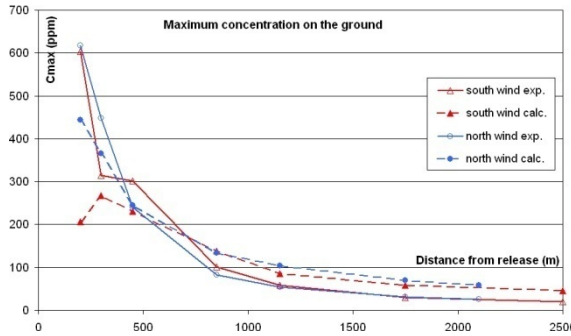


Figure 4. Maximum ground concentration for a release from the containment building

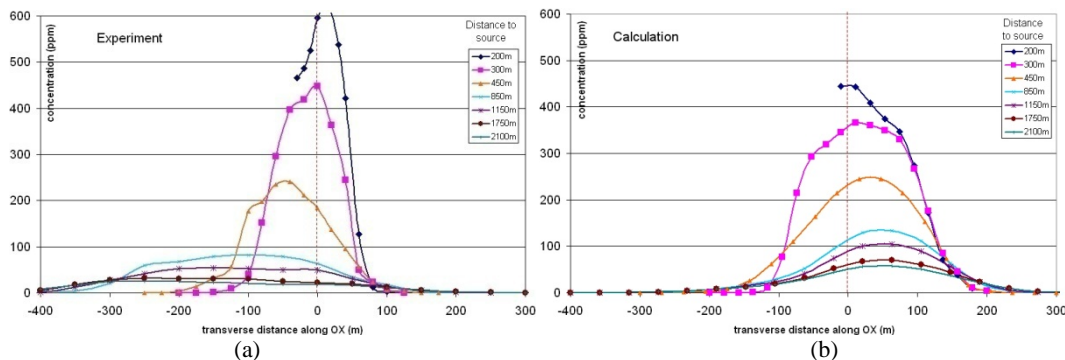


Figure 5. Experimental (a) and computed (b) transverse ground concentration profiles under north wind, release from containment building

Release from the stack

Under south wind, vertical concentration profiles along OY show the plume to be again 10 m higher than measured. The underprediction of the longitudinal velocity V is a likely contribution as it results in underpredicting the horizontal to vertical momentum ratio of the stack exit jet, which affects the initial plume trajectory. The maximum concentration level in the plume at $Y=200$ m is good but then decreases too slowly on the first 500 m when compared with the experiment. Also

diffusion of the plume towards the ground is insufficient. Beyond 1000 m experimental concentrations vary linearly with height and gradually drop down to a few tens of ppm. Consequently ground concentrations are significantly underpredicted upstream of the cooling towers and by compensation overpredicted in their lee by a factor of two (figure 6 and 8). Lastly it is again observed that the lateral plume spread and its diffusion towards the ground are both underevaluated.

Under north wind, the plume altitude is overpredicted by 20 m and its diffusion on the vertical is underpredicted. Consequently the maximum concentration level in vertical profiles is overestimated by a factor of 4 on the first 500 m (figure 6). Similarly the maximum concentration on the ground, although correctly predicted at around 70 ppm, is reached near OY=800 m, that is 400 m too far away from the stack. The result is that ground concentrations are two fold lower than measured upstream this location and twofold higher downstream. Note that whereas the computed plume trajectory remains along the OY axis, the experimental trajectory seems to drift to the right i.e. eastward under south wind (figure 7).

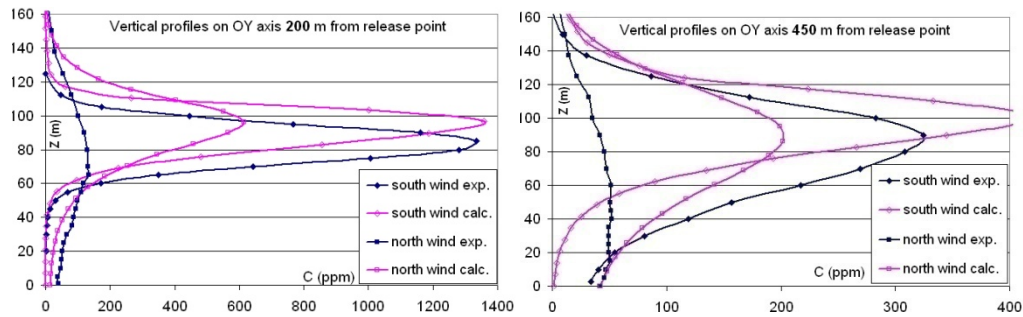


Figure 6. Vertical concentration profiles for the stack release at 2 distances from the source

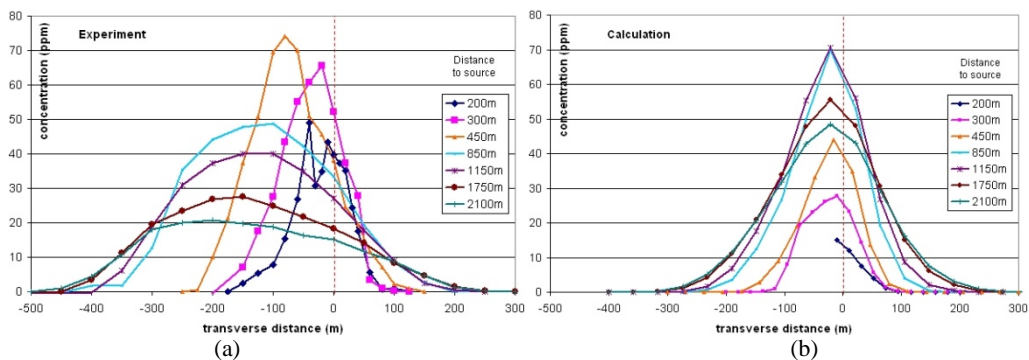


Figure 7. Experimental (a) and computed (b) transverse concentration profiles at ground level under north wind, stack release

Wind tunnel Reynolds number

In an attempt to better simulate the actual conditions in the wind tunnel, the possible effect of the Reynolds number was checked as the Reynolds distortion imposed by the model relatively small scale is close to three orders of magnitude whereas all previous computations were made in full scale conditions.

Although the flow is highly turbulent in the LMFA test section, the model Reynolds number could make the cooling tower regime ($Re=1.8 \cdot 10^7$) go from supercritical in reality to subcritical in the model ($Re=3.6 \cdot 10^4$ less than $Re_c=2$ to $5 \cdot 10^5$), which could result in a widening of their wake. A cooling tower in the planetary boundary layer cannot be strictly assimilated to an infinite cylinder in a uniform flow nevertheless the matter was addressed by rerunning the two stack release cases at the wind tunnel Reynolds number. The velocity field effectively showed some thickening of the decelerated zone downstream the towers, resulting in a significant increase of the ground concentration at the tower foot under south wind (figure 8a); but under north wind the Reynolds distortion has almost no effect as the release is sufficiently far downstream from the towers to be subtracted from their direct influence (figure 8b).

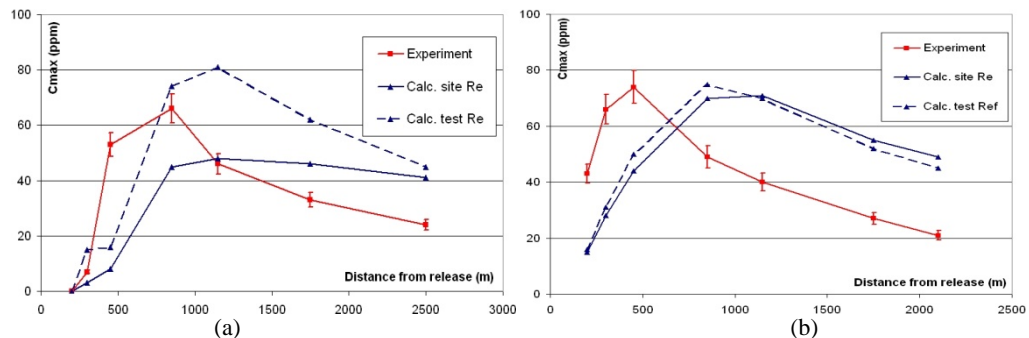


Figure 8. Sensitivity of maximum ground concentration to the Reynolds number under south (a) and north (b) wind

Sensitivity to velocity boundary conditions

Additionally, two boundary parameters were further examined:

- the effect of a hypothetical transverse velocity component in the test section, as a drift of the plume trajectory to the right of the mainstream direction was observed in the experiment, especially under north wind,
- the effect of the stack exit velocity, as the plume altitude was systematically overpredicted by the initial computations.

Under north wind, the following transverse component U was added to match the one actually measured in the test section:

$$U(z) = -0.242 \times (z/50)^{0.17} \text{ ms}^{-1} \text{ for } Z < 50 \text{ m and } U(z) = z/1500 - 0.275 \text{ ms}^{-1} \text{ for } Z > 50 \text{ m} \quad (5)(6)$$

Transverse ground concentration profiles show that the plume drifts westward as expected but it also flows somewhat higher which results in a further reduction of the prediction at ground level compared with the situation without the transverse velocity component.

Figure 9a shows how the plume altitude diminishes when the stack exit velocity is reduced to 75% and 50% respectively of its nominal value. Although this does not suffice to match the much flatter vertical experimental profile, this has a significant effect on the maximum concentration at the ground as evidenced by the series of blue curves on figure 9b. Hence accurately measuring and modelling the stack exit characteristics is of major importance.

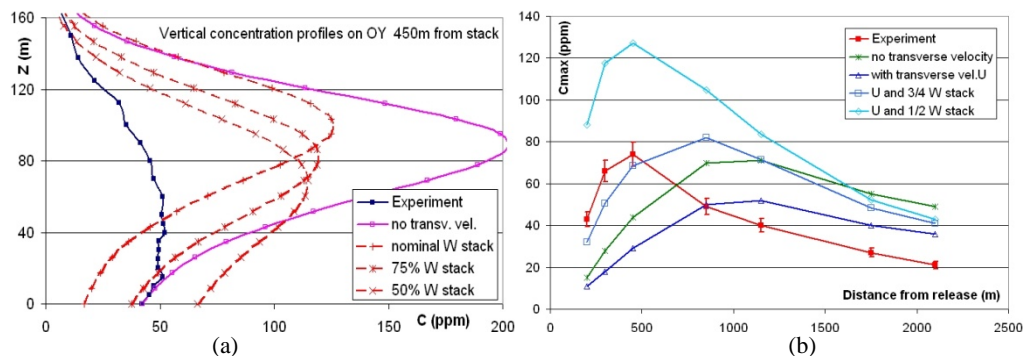


Figure 9. Sensitivity of vertical concentration profiles (a) and maximum ground concentration (b) to lateral wind and stack exit velocity

CONCLUSION

The main characteristics of the concentration field in this simulation of the Bugey site, which depend on the wind direction and gas source location, are qualitatively well captured by the STAR-CD simulation of neutral stability atmospheric dispersion using the standard (k,ϵ) model with the Richards and Hoxey set of boundary conditions. From the quantitative point of view, the ground level concentration is underpredicted on the first hundred metres and conversely overpredicted beyond, which is attributed to the overestimation of the initial plume height by the stack release and underestimation of the downward and lateral plume spread by the (k,ϵ) model. Nevertheless the discrepancy between measurement and prediction is less than a factor of two, which shows that from a practical point of view rather simple CFD modelling can yield useful results for applications in environmental impact or risk management of industrial sites.

REFERENCES

- Blocken, B and T. Stathopoulos, J. Carmeliet, 2007: CFD simulation of the atmospheric boundary layer: wall function problems. *Atmospheric environment* 41, 238-252
- Hargreaves, D.M. and H.G. Wright, 2007: On the use of the $k-\epsilon$ model in commercial CFD software to model the neutral atmospheric, *Journal of Wind Engineering and Industrial Aerodynamics* 95, 355–369
- Launder, B.E. and D.B. Spalding, 1972: *Mathematical models of turbulence*, Academic Press
- Méjean, P. 2003: *Dispersion atmosphérique sur le site de la centrale EDF du Bugey – Essais en soufflerie Laboratoire de Mécanique des Fluides et d'Acoustique, ECL-LMFA-UMR 5509*
- Richards, P.J. and R.P. Hoxey, 1993: Appropriate boundary conditions for computational wind engineering models using the turbulence model. *Journal of Wind Engineering and Industrial Aerodynamics*, 46 & 47, 145-153
- Star-Cd version 3.26: *User Guide and Methodology Manual*. © 2005 CD-Adapco